HHS Public Access

Author manuscript

Neuroimage. Author manuscript; available in PMC 2021 May 01.

Published in final edited form as:

Neuroimage. 2020 May 01; 211: 116627. doi:10.1016/j.neuroimage.2020.116627.

Cortical functional connectivity indexes arousal state during sleep and anesthesia

Matthew I. Banks[1,2,*], **Bryan M. Krause**[1], **Christopher M. Endemann**[1], **Declan I. Campbell**[1], **Christopher K. Kovach**[3], **M. Eric Dyken**[4], **Hiroto Kawasaki**[3], **Kirill V. Nourski**[3,5]

[1]Department of Anesthesiology, University of Wisconsin, Madison, WI, USA

[2]Department of Neuroscience, University of Wisconsin, Madison, WI, USA

[3]Department of Neurosurgery, The University of Iowa, Iowa City, IA 52242, USA

[4]Department of Neurology, The University of Iowa, Iowa City, IA 52242, USA

[5]Iowa Neuroscience Institute, The University of Iowa, Iowa City, IA 52242, USA

Abstract

Disruption of cortical connectivity likely contributes to loss of consciousness (LOC) during both sleep and general anesthesia, but the degree of overlap in the underlying mechanisms is unclear. Both sleep and anesthesia comprise states of varying levels of arousal and consciousness, including states of largely maintained conscious experience (sleep: N1, REM; anesthesia: sedated but responsive) as well as states of substantially reduced conscious experience (sleep: N2/N3; anesthesia: unresponsive). Here, we tested the hypotheses that (1) cortical connectivity will exhibit clear changes when transitioning into states of reduced consciousness, and (2) these changes will be similar for arousal states of comparable levels of consciousness during sleep and anesthesia. Using intracranial recordings from five adult neurosurgical patients, we compared resting state cortical functional connectivity (as measured by weighted phase lag index, wPLI) in the same subjects across arousal states during natural sleep [wake (WS), N1, N2, N3, REM] and propofol anesthesia [pre-drug wake (WA), sedated/responsive (S), and unresponsive (U)]. Analysis of alpha-band connectivity indicated a transition boundary distinguishing states of maintained and

[*]**Corresponding author:** Matthew I. Banks, Ph.D., Professor, Department of Anesthesiology, University of Wisconsin, 1300 University Avenue, Room 4605, Madison, WI 53706, Tel.: (608)261-1143, mibanks@wisc.edu.

Author Contributions

Matthew Banks: conceptualization, methodology, software, validation, formal analysis, investigation, writing – original draft, funding acquisition.

Bryan Krause: methodology, software, formal analysis, data curation, writing – review & editing, visualization.

Christopher Endemann: methodology, software, formal analysis, writing – review & editing, visualization.

Declan Campbell: methodology, software, formal analysis, visualization.

Christopher Kovach: software, data curation, writing – review & editing.

Eric Dyken: formal analysis, writing – review and editing.

Hiroto Kawasaki: investigation, resources.

Kirill Nourski: conceptualization, methodology, software, validation, formal analysis, investigation, investigation, writing – original draft, project administration, funding acquisition.

Competing Interests Statement

The authors declare no competing financial interests.

reduced conscious experience in both sleep and anesthesia. In wake states WS and WA, alpha-band wPLI within the temporal lobe was dominant. This pattern was largely unchanged in N1, REM, and S. Transitions into states of reduced consciousness N2, N3, and U were characterized by dramatic changes in connectivity, with dominant connections shifting to prefrontal cortex. Secondary analyses indicated similarities in reorganization of cortical connectivity in sleep and anesthesia. Shifts from temporal to frontal cortical connectivity may reflect impaired sensory processing in states of reduced consciousness. The data indicate that functional connectivity can serve as a biomarker of arousal state and suggest common mechanisms of LOC in sleep and anesthesia.

Keywords

Alpha-band connectivity; consciousness; intracranial electrophysiology; phase lag index

1. Introduction

Elucidating the changes in the brain that occur upon loss and recovery of consciousness (LOC, ROC) is critical to our understanding of the neural basis of consciousness. It is a prerequisite for improving diagnosis and prognosis of disorders of consciousness, as well as noninvasive monitoring of awareness in clinical settings (Bayne et al., 2017; Bernat, 2017; Stein and Glick, 2016). A primary hurdle is identifying changes that are specific to LOC and ROC, as opposed to nonspecific changes in brain activity in response to endogenous or exogenous factors (e.g. neuromodulators during sleep or anesthetic agents). This can be clarified by investigating common features of LOC and ROC during sleep and anesthesia (Mashour, 2006; Shushruth, 2013; Tung and Mendelson, 2004). A handful of studies have compared the changes in neural activity that occur during transitions between arousal states during sleep versus anesthesia in human subjects (Li et al., 2018; Murphy et al., 2011), but commonalities in neural mechanisms have been elusive, perhaps because sleep and anesthesia data in these studies were obtained in different subjects, or because of the metrics investigated, or both. Here, we compare changes in functional connectivity in the same subjects during sleep and propofol anesthesia.

Although endogenous sleep and arousal centers play a role in initiating changes in arousal state during LOC/ROC (Lydic and Baghdoyan, 2005), these mechanisms likely only partially overlap for sleep and anesthesia (Akeju and Brown, 2017). Importantly, changes in the contents of consciousness are likely secondary to actions in neocortex (Voss et al., 2019), which is the focus of the current study. That is, we sought to identify changes in cortical activity or connectivity that occurred upon LOC, independent of the underlying mechanisms initiating changes in arousal state. Common cortical signatures of LOC under sleep and anesthesia include similar effects of LOC on sensory cortex observed under both conditions. For example, primary sensory cortex is still responsive to environmental stimuli, and basic organizational features such as frequency tuning in auditory cortex are preserved (Nir et al., 2015; Raz et al., 2014), while responses in higher order cortical sensory areas are largely suppressed (Liu et al., 2012; Wilf et al., 2016). In addition, cortical connectivity, which is central to leading theories of consciousness (Dehaene and Changeux, 2011; Friston, 2005;

Tononi et al., 2016), is altered upon LOC during anesthesia (Boly et al., 2012a; Lee et al., 2017; Lee et al., 2013b; Murphy et al., 2011; Ranft et al., 2016; Sanders et al., 2018) and non-rapid eye movement (NREM) sleep (Boly et al., 2012b; Spoormaker et al., 2010).

These studies suggest that LOC under a variety of conditions converges on specific changes in cortical connectivity. However, a major impediment to identifying these changes is a lack of consensus on key details, for example whether overall or long-range connectivity decreases (Boly et al., 2012a; Lee et al., 2013b; Ranft et al., 2016; Spoormaker et al., 2010) or increases (Boly et al., 2012b; Lee et al., 2017; Monti et al., 2013; Murphy et al., 2011) upon LOC. Moreover, despite the evidence for common mechanisms of LOC under anesthesia and during NREM sleep, there are obvious differences between sleep and anesthesia as well (Akeju and Brown, 2017). Specifically, subjects are arousable from the latter but not from the former, and this maintained connectedness with the environment likely involves cortical activation. The structure of natural sleep, in its transitions between REM and multiple stages of NREM sleep, is not mimicked by steady-state anesthesia. A recent imaging study found substantial differences in the changes in functional magnetic resonance imaging (fMRI) functional connectivity that occur during sleep and propofol anesthesia (Li et al., 2018). Slow wave components of EEG signals during sleep and anesthesia in animal models exhibit distinct patterns of activity as well (MacIver and Bland, 2014). Furthermore, delta-band activity during the deepest stages of NREM sleep (N3) most closely resembles brain activity under anesthesia (Murphy et al., 2011), but unresponsiveness (and presumably reduced level of consciousness) occurs as well in stage 2 NREM (N2) sleep (Strauss et al., 2015). Direct comparisons of changes in connectivity associated with LOC under natural sleep and anesthesia may help resolve these discrepancies.

Here, we investigated changes in cortical functional connectivity across arousal states under natural sleep and anesthesia. Intracranial recordings obtained from neurosurgical patients with pharmacologically resistant epilepsy allowed us to compare connectivity using data obtained from the same recording sites in the same subjects.

2. Materials and Methods

2.1. Subjects

Experiments were carried out in five neurosurgical patients diagnosed with medically refractory epilepsy who were undergoing chronic invasive electrophysiological monitoring to identify seizure foci prior to resection surgery (Supplementary Table 1). Research protocols were approved by the University of Iowa Institutional Review Board and the National Institutes of Health, and written informed consent was obtained from all subjects. Research participation did not interfere with acquisition of clinically necessary data, and subjects could rescind consent for research without interrupting their clinical management. Subjects were right-handed, left language-dominant native English speakers. All subjects underwent standard neuropsychological assessment prior to electrode implantation, and none had cognitive deficits that would impact the results of this study. The subjects were tapered off their antiepileptic drugs (AEDs) during chronic monitoring when overnight sleep data were collected (see below). All subjects had their medication regimens reinstated at the

end of the monitoring period, prior to induction of general anesthesia for the resection surgery.

2.2. Experimental procedures

Electrocorticographic (ECoG) recordings were made using subdural and depth electrodes (Ad-Tech Medical, Racine, WI). Subdural arrays consisted of platinum-iridium discs (2.3 mm diameter, 5–10 mm inter-electrode distance), embedded in a silicon membrane. Depth arrays (8–12 electrodes, 5 mm inter-electrode distance) were stereotactically implanted along the anterolateral-to-posteromedial axis of Heschl's gyrus (HG). Additional arrays targeted insular cortex and provided coverage of planum temporale and planum polare. This allowed for bracketing suspected epileptogenic zones from dorsal, ventral, medial, and lateral aspects (Nagahama et al., 2018; Reddy et al., 2010); Supplementary Fig. 1). Depth electrodes also targeted amygdala and hippocampus, and provided additional coverage of the superior temporal sulcus. A subgaleal electrode, placed over the cranial vertex near midline, was used as a reference in all subjects. All electrodes were placed solely on the basis of clinical requirements, as determined by the team of epileptologists and neurosurgeons (Nourski and Howard, 2015).

Two sets of no-task, resting-state (RS) data were recorded: overnight sleep data were collected first, followed several days later by anesthesia data. RS ECoG, EEG, and video data were collected from subjects during natural overnight sleep (Supplementary Fig. 2a). Sleep data were collected in the dedicated, electrically shielded suite in The University of Iowa Clinical Research Unit while the subjects lay in the hospital bed. Sleep data were collected 6 days after ECoG electrode implantation surgery in subjects L372, R376 and L403, 7 days after surgery in subject L423, and 8 days after surgery in subject L409. Data were recorded using a Neuralynx Atlas System (Neuralynx Inc., Bozeman, MT), amplified, filtered (0.1–4000 Hz bandpass, 12 dB/octave rolloff), sampled at 16 kHz.

Stages of sleep were defined manually using facial EMG and scalp EEG data based on standard clinical criteria (Berry et al., 2017) independently by two individuals who participate in the inter-scorer reliability program of the American Academy of Sleep Medicine: a licensed polysomnography technologist, certified by the Board of Registered Polysomnography Technologists, and a physician certified in Sleep Medicine by the Accreditation Council for Graduate Medical Education. The final staging report was agreed upon by the two scorers after a collaborative review. Scalp and facial electrodes were placed by an accredited technician, and data were recorded by a clinical acquisition system (Nihon Kohden EEG-2100) in parallel with research data acquisition. Facial electrodes were placed following guidelines of the American Academy of Sleep Medicine (Berry et al., 2017) at the left and right mentalis for EMG, and adjacent to left and right outer canthi for EOG. EEG was obtained from electrodes placed following the international 10–20 system at A1, A2, F3, F3, F4, O1, and O2 in all subjects, with the following additional electrodes: C3 and C4 in all subjects but R376; E1 and E2 in L372 and R376; CZ and FZ in L409 and L423; and F8 in L423. All subjects had periods of REM, N1 and N2 sleep identified; three out of five subjects had N3 sleep periods as well. One subject (L403) experienced multiple seizures in the second half of the night; those data were excluded from analysis. The durations of

recordings for each sleep stage in each subject are provided in Supplementary Table 2; all data were used in the analyses.

Anesthesia RS data were collected in the operating room prior to electrode removal and seizure focus resection surgery (6 days after collection of overnight sleep data in subject L409, 7 days in subjects L372 and L423, and 8 days in subjects R376 and L403). Data were recorded using a TDT RZ2 processor (Tucker-Davis Technologies, Alachua, FL), amplified, filtered (0.7–800 Hz bandpass, 12 dB/octave rolloff), and digitized at a sampling rate of 2034.5 Hz. We note that the highpass cutoff frequency on this hardware precluded analysis of frequencies below 1 Hz. Although no specific instructions were given about keeping eyes open or closed, subjects were observed to have eyes closed during nearly all resting state recordings. Data were recorded in 6-minute blocks, interleaved with an auditory stimulus paradigm as part of a separate study (Nourski et al., 2018a, b). Data were collected during an awake baseline period and during induction of general anesthesia with incrementally titrated propofol infusion (50 – 150 μg/kg/min; Supplementary Fig. 2b).

Awareness was assessed using the Observer's Assessment of Alertness/Sedation (OAA/S) scale (Chernik et al., 1990) and using bispectral index (BIS) (Gan et al., 1997) using BIS Complete 4-Channel Monitor (Medtronic plc, Minneapolis, MN). OAA/S was assessed just before and just after collection of each RS data block. Wake state (WA) and two levels of anesthesia (arousal states) were targeted: sedated but responsive to command (S; OAA/S ≥ 3) and unresponsive (U; OAA/S ≤ 2) (Nourski et al., 2018a). Estimated plasma propofol concentrations were calculated on a minute-by-minute basis for each subject based on their age, weight, gender, and propofol infusion rate using a pharmacokinetic model (Schnider et al., 1998).

In four of five subjects, OAA/S values crossed the boundary between S and U over the course of the 6-minute RS block (e.g. RS block #1 in subject L372; see Supplementary Fig. 2b). In these cases, only the first and last 60-second segments of the block were analyzed; data from the first segment were assigned to the S state, and data from the second segment were assigned to the U state. BIS data were recorded continuously throughout the experiment and were manually logged on a minute-by-minute basis. BIS was summarized as median values for each of the three states (WA, S, and U) as well as median values immediately prior to and following each OAA/S assessment. The durations of recordings for each arousal state during the anesthesia experiment in each subject are provided in Supplementary Table 2; all data were used in the analyses.

2.3. Data analysis

2.3.1. Band power analysis—Data were assigned to specific arousal states based on sleep scoring and OAA/S assessment. For each subject, sleep and anesthesia data were divided into segments of length 60 seconds for all analyses except the classification analysis (see Fig. 5 below), for which 10-second segments were used. Time-frequency analysis was performed using the demodulated band transform (DBT; Kovach and Gander, 2016), which optimizes frequency resolution for each frequency band specified, while minimizing spectral leakage across bands. PSDs were estimated for each data segment from the squared magnitude of the DBT. For each subject, PSDs were averaged across segments assigned to

identical arousal states. ECoG band power was calculated as the average power across frequency in each band. Band power within ROI group was computed as the average across all recording sites in that ROI group, and arousal state-dependent changes in band power were evaluated using linear mixed effects models as follows. The data were normalized to total power and log transformed, then fit with a model incorporating fixed effects of state, ROI, and the interaction of state and ROI, and random effects for channels nested within subjects and with random slopes for brain state by subject, using the R package lme4 (Bates et al., 2015). Estimated marginal means and 95% CIs for each ROI and state were calculated, as well as pairwise between-states contrasts within each ROI with *p*-values adjusted by multivariate *t* for all comparisons within a band, using the R package emmeans (Lenth, 2019).

2.3.2. Connectivity analysis—Connectivity was measured using the debiased weighted phase lag index (wPLI) (Vinck et al., 2011), a non-directed measure of phase synchronization that eschews synchronization near zero phase lag to avoid artifacts due to volume conduction. For each data segment, wPLI was estimated for every electrode pair from the sign of the imaginary part of the DBT-derived cross-spectrum at each frequency and averaged across frequencies within each band of interest (delta: 1–4 Hz, theta: 4–8 Hz, alpha: 8–13 Hz, beta: 13–30 Hz, gamma: 30–70 Hz; high gamma: 70–120 Hz). As the analysis results tended to be correlated in the frequency domain, we chose to present only the results for the delta, alpha and gamma band. Alpha-band wPLI in particular is a commonly used measure of functional connectivity (Blain-Moraes et al., 2014; Blain-Moraes et al., 2015; Lee et al., 2013a; Lee et al., 2017; van Dellen et al., 2014). In addition, we observed evidence for alpha-band oscillatory components in the resting state power spectra, further motivating focus on this band. Therefore, our primary measure of functional connectivity was alpha-band wPLI, but connectivity in delta and gamma bands is presented as well for comparison.

2.3.3. Anatomical reconstruction and ROI parcellation—Electrode localization relied on post-implantation T1-weighted structural MR images and post-implantation CT images. All images were initially aligned with pre-operative T1 images using linear coregistration implemented in FSL (FLIRT) (Jenkinson et al., 2002). Electrodes were identified in the post-implantation MRI as magnetic susceptibility artifacts and in the CT as metallic hyperdensities. Electrode locations were further refined within the space of the pre-operative MRI using three-dimensional non-linear thin-plate spline warping (Rohr et al., 2001), which corrected for post-operative brain shift and distortion. The warping was constrained with 50–100 control points, manually selected throughout the brain, which aligned to visibly corresponding landmarks in the pre- and post-implantation MRIs.

To compare functional connectivity between arousal states, the dimensionality of the adjacency matrices (i.e. the wPLI connectivity matrices) was reduced by assigning electrodes to one of 37 specific ROIs organized into 7 ROI groups (see Fig. 3; Table 1; Supplementary Table 3) based upon anatomical reconstructions of electrode locations in each subject. For subdural arrays, it was informed by automated parcellation of cortical gyri (Destrieux et al., 2010; Destrieux et al., 2017) as implemented in the FreeSurfer software

package. For depth arrays, ROI assignment was informed by MRI sections along sagittal, coronal, and axial planes. For recording sites in HG, delineation of core auditory cortex and adjacent non-core areas (HGPM and HGAL, respectively) was based on physiological criteria (Brugge et al., 2009; Nourski et al., 2016). Specifically, recording sites were assigned to the HGPM ROI if they exhibited phase-locked ECoG responses to 100 Hz click trains and if the averaged evoked potentials to these stimuli featured short-latency (<20 ms) components. Such response features are not present within HGAL. Additionally, correlation coefficients between average evoked potential waveforms recorded from adjacent sites were examined to identify discontinuities in response profiles along HG that could be interpreted as reflecting a transition from HGPM to HGAL. Recording sites identified as seizure foci or characterized by excessive noise, and depth electrode contacts localized to the white matter or outside brain, were excluded from analyses and are not listed in Supplementary Table 3.

2.3.4. ROI-based connectivity analysis—Connectivity between ROIs was computed as the average wPLI value between all pairs of recording sites in the two ROIs. For analyses in which connectivity was summarized across subjects (see Fig. 4 and Supplementary Figs. 6 & 7), ROIs were only included if at least 3 out of 5 subjects had electrode coverage in that ROI; 29 out of 37 ROIs met this criterion. For all other analyses, data from all ROIs, including those contributed by fewer than three subjects, were used. For display purposes only, adjacency matrices for each subject were averaged across segments assigned to identical arousal states, and the matrices thresholded to retain only the 10% strongest connections. All quantitative analyses were based on unthresholded adjacency matrices.

Changes in connectivity with arousal state were evaluated by computing differences between adjacency matrices, and quantified by calculating the operator norm (d) of the difference matrix; smaller values of d indicate more similar matrices. This difference metric was chosen instead of either the Pearson correlation or the Frobenius norm because it retains information about the structure of the matrix. Specifically, for a matrix $\mathbf{M}$, d_M is the maximum, over all vectors $\mathbf{v}$ with $||\mathbf{v}|| = 1$, of $||\mathbf{Mv}||$, and indicates how much $\mathbf{M}$ stretches these vectors; with $\mathbf{M}$ representing the difference between adjacency matrices measured in two arousal states, $\mathbf{v}$ could represent the inputs to or the activity of the nodes of the network at a particular time point, and $\mathbf{Mv}$ would then be the effect on that activity of the difference in brain state. The operator norm [computed in Matlab as norm ($\mathbf{M}$)] is related to the spectrum of $\mathbf{M}^T\mathbf{M}$: d_M = the square root of the maximum eigenvalue of $\mathbf{M}^T\mathbf{M}$.

To compare arousal state-dependent differences in d (for example, to see whether $d_{WS,N1}$ is different than $d_{N1,N2}$), effect sizes were calculated as Cliff's delta, δ (Cliff, 1993). Cliff's delta ranges from -1 to 1 where 0 indicates completely overlapping distributions, and -1 or 1 indicate distributions where all observed values of one group are less/greater than all observed values of the comparison group. Effect sizes were first calculated for each subject, and then reported as the mean effect size across subjects, $\bar{\delta}$. A permutation method was used to estimate p-values for these comparisons; within each subject and each experiment (sleep and anesthesia), restricted random permutations of state labels for the data segments, preserving the order of observations, produced an estimated distribution under the null hypothesis that the comparisons do not depend on arousal state (Besag and Clifford, 1989;

Winkler et al., 2015). Independent *p*-values obtained within individual subjects for a given test were combined across subjects using Stouffer's *Z*-transform method (Heard and Rubin-Delanchy, 2018; Stouffer et al., 1949). Non-parametric approaches (Cliff's delta and permutation method) were preferable to parametric statistics for these data, as the distributions of operator norms and differences were skewed, and the magnitude varied between subjects. Given the small number of subjects, these statistical methods treat each subject as a single-case and then combine results in a meta-analysis. Because *p*-values and effect sizes were first estimated in single subjects, this approach reduces the influence of possible outlier subjects and non-normally distributed measures.

2.3.5. Classification analysis—We used a classification analysis as an additional evaluation of changes in connectivity as a function of arousal state. Here, data from each subject was divided into 10-second segments, and adjacency matrices were computed for each segment. To ensure that the data from the two experiments (sleep and anesthesia) were on the same scale, adjacency matrices computed from the anesthesia data were scaled by the slope derived from a regression analysis that related wPLI values computed for sleep vs. anesthesia data for each subject. A linear classifier (implemented using SGDClassifier from Python's Scikit-Learn library) was trained on a subset (80%) of WS and N2 segments, and then applied to unseen data from all arousal states (WS, N1, N2, N3, REM, WA, S, U) in each subject. Models were trained on data from the sleep experiment because there were many more segments available compared to anesthesia (see Supplementary Fig. 2). Given an unequal number of segments in WS and N2 stages (see Supplementary Table 2), training sets were balanced via random sampling. Rather than using a binary classification scheme, we assigned each segment a prediction score from 0 (most 'N2-like') to 1 (most 'WS-like') via logistic regression. We report the median logistic prediction scores across all 750 model permutations (25 pairwise permutations of WS and N2 train/test splits (4/5 train, 1/5 test) in each subject; 30 random shuffles of each pre-balanced training dataset). A tolerance threshold (i.e. when to stop training a given model) hyperparameter was optimized for each training set permutation using three-fold cross-validation. Specifically, each training set was split into three folds, and one of those three folds was used to evaluate the performance of a given hyperparameter value. For each hyperparameter value evaluated, this process was repeated three times to average over all (hyperparameter) test sets. The hyperparameter value yielding the lowest average test set error was then used in the final model applied to unseen data for each train/test permutation. Probability density functions for each arousal state and each subject were estimated from logistic prediction scores using kernel density estimation (ksdensity function in Matlab) and are represented as violin plots (see Fig. 5 and Supplementary Fig. 8).

2.3.6. Regional connectivity analysis—State-dependent differences in regional connectivity were quantified by dividing ROIs into a posterior ('back') group [temporal (HGPM, HGAL, PT, PP, STGA, STGM, STGP, Ins, STS, MTGP, MTGM, MTGA, ITG, PHG, FG, TP), parietal (AG, SMG, PostCG, SPL), and occipital (IOG, MOG) ROIs], and an anterior ('front') group [i.e. frontal ROIs (IFGop, IFGtr, IFGor, MFG, SFG, CGA, OG, TFG, PreCG, PMC, LG, CGM, GR) as well as Amyg and Hipp]. Mean alpha-band wPLI across all pairs of recording sites within each group were used to calculate bias in

connectivity, defined as the difference between within-posterior and within-anterior connectivity. State-dependence of long-range alpha-band connectivity was assayed by measuring wPLI across the top 25% most distant pairs of recording sites. Euclidean distances between sites were measured using standard 3D coordinates (Right-Anterior-Superior, RAS). Changes in within-posterior versus within-anterior connectivity and changes in long-range connectivity were assessed using permutation analysis as described above for state-dependent differences in *d*.

3. Results

3.1. Electrode coverage

Data from a total of 864 recording sites from five subjects (Supplementary Table 1), spanning a total of 37 regions of interest (ROIs) were analyzed (Table 1). Each subject contributed between 154 and 198 sites (median 172; Supplementary Table 3, Supplementary Fig. 1). The focus of this study was on changes in cortical connectivity across arousal states. As sensory awareness is a key element of consciousness (Boly et al., 2017), we centered our analysis around cortical hierarchical organization in the auditory modality, which is a convenient choice and a frequent focus of studies of both sleep and general anesthesia (e.g. (Liu et al., 2012; Raz et al., 2014; Strauss et al., 2015). Clinical considerations dictated dense sampling of the temporal lobe, including auditory and auditory-related cortex, providing comprehensive electrode coverage across multiple levels of the auditory cortical hierarchy in all subjects.

3.2. Defining arousal states

Polysomnography based on scalp electroencephalography (EEG), electrooculography, electromyography, and video was used to assign sleep stages. All five subjects exhibited overnight sleep patterns typical of healthy adult subjects (Supplementary Fig. 2a). There was a high correspondence between the ratio of delta to beta band power in frontal ECoG electrodes and the assigned sleep stage (cf. Kremen et al., 2019). Overnight recordings in all subjects featured wake (WS) state as well as N1, N2, and REM sleep stages; N3 was also observed in 3 of 5 subjects (Supplementary Table 2). The total duration of scored recordings in each subject was between 284 and 584 minutes (median 481 minutes).

During the anesthesia experiment, all subjects transitioned from wake (WA) to sedated (S; OAA/S>2) and unresponsive (U; OAA/S ≤2) states as propofol infusion rate was increased (Supplementary Fig. 2b). Average estimated plasma propofol concentration at loss of responsiveness was 2.31 μg/ml (range 1.71–3.01 μg/ml). OAA/S scores exhibited a good correspondence with bispectral index (BIS) values, as expected for sedation and anesthesia induced by propofol alone (Glass et al., 1997). WA, S, and U states were characterized by average median BIS values of 92 (range of medians across the five subjects 83–98), 77.5 (range 45–88) and 45 (range 41–68), respectively.

OAA/S assessments depend on subjects responding to a simple command, and thus have the potential themselves to alter arousal state. To determine whether this happened in these experiments, we compared BIS values recorded before and after the 23 OAA/S assessments

that were proximal to the resting state recording blocks whose data are presented here. In 19/23 assessments, we saw minimal changes in BIS (range [−8 10]; median pre-assessment BIS=72; median post-assessment BIS=73); in the other four we saw large changes but in either direction (increases of 21, 41 and 39, and a decrease of 46). Thus, in the majority of cases, administering the OAA/S did not substantively change arousal state. Overall, increases in BIS values immediately following OAA/S assessment failed to reach significance (median pre-assessment BIS = 70; median post-assessment BIS = 74; $p = 0.18$, one-tailed Wilcoxon signed rank test).

3.3. Changes in spectral power under sleep and anesthesia

Power spectral density (PSD) measurements made during WS and WA states exhibited shapes typical of resting state eyes-closed recordings, with power falling off approximately as $1/f^2$ and broad peaks typically observed in the alpha and beta bands (Fig. 1; Supplementary Fig. 3). There were only small differences observed between WS and N1, and none between WA and S (Fig. 2). By contrast, transitions into states N2 and U were characterized by large band- and region-specific changes in PSDs. As expected, N2 sleep was characterized by a widespread increase in delta power (see Fig. 2a). Of note, increases in alpha power in N2, as might be expected due to sleep spindles (Andrillon et al., 2011), were not consistent across subjects. Loss of responsiveness under anesthesia (U) was associated with large increases in delta power within PFC and sensorimotor areas, and a selective increase in alpha power in PFC (see Fig. 2b), consistent with previous observations (Purdon et al., 2013).

3.4. Changes in functional connectivity under sleep and anesthesia

It is clear from the differences between the sleep and anesthesia data shown in Figures 1 and 2 that changes in spectral power alone are unlikely to serve as a generalized biomarker for LOC in the two sets of arousal states. We sought instead to investigate whether such biomarkers could be found in analyses of cortical connectivity. Functional connectivity was assayed using the debiased weighted phase lag index (wPLI) (Vinck et al., 2011). As ECoG power spectra featured peaks in the alpha band, we focused on alpha-band wPLI, but presented analyses of functional connectivity in other canonical frequency bands as well.

Adjacency matrices were computed first for each pair of recording sites (Fig. 3a), then transformed into ROI-based adjacency matrices (Fig. 3b), from which chord connectivity plots were created (Fig. 3c). Single-subject examples of chord connectivity plots for delta, alpha, and gamma bands across arousal states during sleep and anesthesia are shown in Supplementary Figures 4 and 5. On average, in the wake states (WA, WS) the strongest connections in the alpha-band were within the temporal lobe (Fig. 4). This pattern was largely preserved in N1, REM and S states. By contrast, a distinct connectivity profile emerged for N2 and U, in which the strongest alpha-band connections were within prefrontal cortex and between prefrontal cortex and select ROIs, including insula, gyrus rectus, and PMC (see Fig. 4, third column). More modest changes in connectivity were observed in other frequency bands (Supplementary Fig. 6). In the three subjects in whom N3 sleep was observed, the shift in alpha-band connectivity was even more pronounced in N3 compared to N2 (Supplementary Fig. 7).

The wPLI is in theory insensitive to changes in spectral power in the underlying signals (Vinck et al., 2011). However, like other phase-related measures, wPLI can be sensitive to uncorrelated noise (Vinck et al., 2011), leading to correlations with spectral power in real-world recordings. To explore this issue in the data presented here, it was important to control for arousal state, as changes in both spectral power and wPLI were associated with changes in arousal state, but these changes might be independent of each other. Thus, we investigated the relationship between power and wPLI in each data segment and at each recording site separately for each arousal state. If changes in spectral power drive changes in wPLI, a correlation between these measurements should have been observed. However, in the dataset presented here power did not exhibit an appreciable correlation with wPLI residuals (mean across patients $R^2 = 0.02$, maximum $R^2 = 0.04$) after accounting for arousal state, indicating that spectral power changes did not contribute substantially to our measure of functional connectivity.

3.5. Common neural signature of functional connectivity changes in sleep and anesthesia

A striking transition boundary in the alpha-band connectivity patterns between two sets of arousal states – [WS, N1, REM, WA, S] and [N2, N3, U] – is apparent visually in the chord connectivity plots of Figure 4. Differences in the degree of conscious experience in these two sets suggest a functional boundary as well: the first set comprises states in which subjects were responsive (WS, WA, S), or had high incidence of reportable conscious experience within the context of dreaming (N1, REM), while the second set comprises states in which subjects were unresponsive and had low incidence of reportable conscious experience (Eer et al., 2009; Leslie et al., 2009; Siclari et al., 2013). However, we note that Figure 4, while visually striking, is an abstraction from the data both because it is an average across subjects and because it displays only the 10% strongest connections.

To confirm the existence of a transition boundary, we applied two different analyses. First, changes in connectivity with arousal state were measured using the differences between un-thresholded ROI × ROI adjacency matrices. Specifically, the magnitude of the difference in connectivity between states J and K was computed as $d_{J,K} = ||\mathbf{A}_J - \mathbf{A}_K||$, where $\mathbf{A}$ is the adjacency matrix for that state and $||\mathbf{M}||$ is the operator norm of the matrix $\mathbf{M}$ (see Methods). Using this metric, functional connectivity was evaluated within each experiment (sleep, anesthesia) to test the hypothesis that differences across the transition boundary (sleep: $d_{N1,N2}$ and $d_{REM,N2}$; anesthesia: $d_{S,U}$) were larger in magnitude than differences that do not cross that boundary (sleep: $d_{WS,N1}$, $d_{WS,REM}$; anesthesia: $d_{WA,S}$). Mean effect sizes across subjects (mean Cliff's delta, $\bar{\delta}$, see methods) are reported, and a permutation test was performed to estimate how chance arrangements of the data compare to the actual differences observed. We found that within the alpha-band, $d_{WS,N1}$ was significantly smaller than $d_{N1,N2}$ ($\bar{\delta} = 0.36$, $p = 0.0012$), as was $d_{WA,S}$ compared to $d_{S,U}$ ($\bar{\delta} = 0.70$, $p = 0.045$). Additionally, $d_{WS,REM}$ was significantly smaller than $d_{REM,N2}$ ($\bar{\delta} = 0.29$, $p = 0.0016$). Comparable results (i.e. both $d_{WS,N1} < d_{N1,N2}$ and $d_{WA,S} < d_{S,U}$ significant) were not found within delta and gamma bands (Supplementary Fig. 6; Supplementary Table 4).

Further support for a transition boundary distinguishing alpha-band connectivity profiles was provided by classification analysis (Fig. 5a). Rather than starting with the average connectivity profiles, as in the difference norms analysis above, the classification analysis was based directly on the time series of connectivity matrices measured during the overnight sleep experiment. The classifier was trained on data segments from two states appearing to fall on either side of the boundary, WS and N2, and then tested on data segments from all arousal states. We used a logistic weighting function to assign a value between 0 ('N2-like') and 1 ('WS-like') to each segment. For this analysis, adjacency matrices were calculated from shorter (10-second) segments of data to provide a larger dataset on which to train the classifier, and the analysis was performed on each subject separately. As expected, median prediction scores on N2 and WS were highly skewed toward 0 and 1, respectively (N2: 0.045; WS: 0.95). Separation in median prediction score for N2 and WS segments was greater for alpha (difference of medians = 0.91) compared to other frequency bands (delta, difference of medians = 0.54; gamma, difference of medians = 0.49). N3 data were classified as 'N2-like' (median logistic prediction score = 0.028). Importantly, both N1 and REM tended to be classified as 'WS-like' (median logistic prediction score = 0.68 and 0.66, respectively). Overall, classification results were generally consistent across the five subjects (Supplementary Fig. 8). An examination of the time series of prediction scores over the duration of the sleep experiment in each subject provided additional evidence for robustness of the classifier performance (Supplementary Fig. 9). Specifically, prediction scores were generally consistent over time for each arousal state, and exhibited rapid transitions associated with changes in arousal state in individual subjects.

The similarities between connectivity profiles measured during sleep and anesthesia (i.e. between WS and WA, between N1 and S, and between N2 and U; Fig. 4) suggest a commonality in the changes in cortical network organization secondary to transitions between arousal states in the two experiments. This observation is consistent with our prior expectation that arousal states associated with similar degrees of conscious experience during sleep and anesthesia ('equivalent states': WS and WA, N1 and S, N2 and U) would have more similar network organization than their 'non-equivalent' counterparts (i.e., those on opposite sides of the transition boundary in Fig. 4). To test this hypothesis, the distances between alpha-band connectivity profiles measured in 'equivalent' versus 'non-equivalent' states were compared; that is, d_{Equiv} (i.e. $d_{WS,WA}$, $d_{N1,S}$ and $d_{N2,U}$) were compared to $d_{Non\text{-}equiv}$ [i.e. mean ($d_{WS,U}$,$d_{WA,N2}$), mean ($d_{N1,U}$, $d_{S,N2}$) and mean ($d_{N1,U}$, $d_{S,N2}$), respectively]. We found that $d_{WS,WA}$ and $d_{N1,S}$ were significantly smaller than their corresponding $d_{Non\text{-}equiv}$ ($\bar{\delta} = 0.22$, $p = 0.0037$ and $\bar{\delta} = 0.22$, $p = 0.00069$, respectively) but $d_{N2,U}$ was not ($\bar{\delta} = 0.13$, $p = 0.34$). These data indicate similarity in alpha-band connectivity profiles observed during N1 sleep and sedation. Comparable results (i.e. both $d_{WS,WA}$ and $d_{N1,S}$ significantly smaller than their corresponding $d_{Non\text{-}equiv}$) were not found within delta and gamma bands (Supplementary Fig. 6; Supplementary Table 4).

Classification analysis also provided support for the idea that connectivity profiles under sleep and anesthesia overlap. Here, classifiers trained on WS and N2 data from the sleep experiment (see Fig. 5a) were applied to anesthesia data (Fig. 5b) in order to determine whether the transition boundary observed during sleep generalized to changes in arousal

state under anesthesia. The classifiers tended to assign WA segments to the WS-like category (median logistic prediction score = 0.70), and assigned U segments with high probability to the N2-like category (median logistic prediction score = 0.078). By contrast, S segments were equally likely to be assigned to WS and N2 (median logistic prediction score = 0.50). The former result stands in contrast to the result of the difference norms analysis that did not reveal a greater similarity between N2 and U compared to other states. Overall, classification results of anesthesia data were generally consistent across subjects and over the duration of each experiment in individual subjects (see Supplementary Figures 8, 9). The classifier results suggest substantial overlap in connectivity profiles between some 'equivalent' sleep and anesthesia arousal states, while connectivity in S bears similarity to both WS and N2 states.

3.6. Regional distribution of functional connectivity strength across arousal states

The changes in regional distribution of connectivity across the transition boundary suggested by the results of Figure 4, i.e. the shift from temporo-parietal to prefrontal connectivity, were strikingly similar in the sleep and anesthesia experiments (see Fig. 4). Boly and colleagues ((Boly et al., 2017) presented evidence that the neural correlates of consciousness correspond primarily to activity in the 'back' of the brain, specifically involving broad regions in the temporal, parietal and occipital lobes, and excluding regions in the frontal lobe. Motivated by this perspective, we quantified the differences in regional connectivity observed across arousal states in the current study. We divided ROIs into two groups: a posterior group that included all temporal, parietal and occipital ROIs, and an anterior group that included all frontal ROIs. We then compared the mean alpha-band wPLI across all pairs of recording sites within each group, and calculated a regional bias in connectivity as the difference between within-anterior and within-posterior connectivity. Figure 6a shows the bias in connectivity, with biases toward within-posterior connectivity indicated by negative values and within-anterior by positive values. There was a shift from posterior and towards anterior connectivity with reduced arousal in both sleep [change in regional bias from N2-N1 $\bar{\delta} = 0.71$, $p < 0.0001$; N2-WS $\bar{\delta} = 0.73$, $p < 0.0001$] and anesthesia (U-S $\bar{\delta} = 1.0$, $p = 0.013$; U-WA $\bar{\delta} = 1.0$, $p = 0.0003$). The shift from WS to N1 or WA to S was not significant (N1-WS $\bar{\delta} = 0.37$, $p = 0.070$; S-WA $\bar{\delta} = 0.98$, $p = 0.056$). REM was different from N2 (N2-REM $\bar{\delta} = 0.83$, $p < 0.0001$) but not significantly different from wake (REM-WS $\bar{\delta} = 0.20$, $p = 0.39$). An examination of the time series of alpha wPLI regional bias over the experiment duration in each subject provided additional evidence for association between a shift towards anterior connectivity and states of reduced consciousness (Supplementary Fig. 10). Specifically, four out of five subjects (L372, R376, L403, L409) exhibited shifts toward anterior connectivity that were unique to unresponsive states (N2 and N3), while REM and N1 segments remained similar to WS in terms of wPLI regional bias. Notably, in all five subjects, U was characterized by shift toward anterior connectivity bias. Thus, the data indicate that alpha-band connectivity in WS versus N2 and in WA versus U exhibits a similar shift from connectivity within posterior towards connectivity within anterior regions.

Finally, disruption in long-range cortico-cortical connectivity has been noted upon LOC during sleep and anesthesia in several studies (Boly et al., 2012a; Lee et al., 2013b; Ranft et al., 2016; Spoormaker et al., 2010), though these findings have been challenged by other

studies (Boly et al., 2012b; Lee et al., 2017; Monti et al., 2013; Murphy et al., 2011). To investigate this issue in the dataset presented here, we assayed the state-dependence of long-range alpha-band connectivity by measuring wPLI across the most distant pairs of recording sites, defined as highest quartile of Euclidean distances in each subject (Fig. 6b). We found no evidence for a decrease in long-range functional connectivity, observing rather a modest increase in N2 and U relative to wake (N2-WS $\bar{\delta} = 0.57$, $p < 0.0001$; U-WA $\bar{\delta} = 0.73$, $p = 0.0053$) and N1/S (N2-N1 $\bar{\delta} = 0.64$, $p < 0.0001$; U-S $\bar{\delta} = 0.86$, $p = 0.0050$). We did not find significant changes in long-range connectivity between WS and N1 (N1-WS $\bar{\delta} = -0.21$, $p = 0.15$) or WA and S (S-WA $\bar{\delta} = -0.05$, $p = 0.57$), but long-range connectivity was reduced in REM (R-WS $\bar{\delta} = -0.79$, $p = 0.00063$).

4. Discussion

The search for reliable biomarkers of LOC/ROC is of great scientific interest and clinical relevance for anesthesia (Drummond, 2000) as well as for diagnosis and prognosis of disorders of consciousness (Bayne et al., 2017; Bernat, 2017). Here, we leveraged a unique opportunity to obtain intracranial electrophysiological recordings from neurosurgery patients both during natural sleep and under propofol anesthesia. We found that different arousal states were associated with distinct patterns of functional connectivity. Similarities in this association for sleep and anesthesia suggest that cortical network configuration could index changes in consciousness.

4.1. ROI- and band-specific effects of sleep and anesthesia on power spectral density

A practical biomarker of conscious vs unconscious state must generalize to multiple settings where LOC is encountered, including sleep and general anesthesia. Previous attempts to use band-specific power to distinguish arousal states under general anesthesia have been largely unsuccessful (Otto, 2008; Struys et al., 1998). This difficulty likely stems from agent-specific changes in power spectra, for example differing between propofol, ketamine and dexmedetomidine anesthesia (Mashour, 2020). The changes that we observed during natural sleep, specifically widespread increases in spectral power in the delta band (see Fig. 2a), are hallmarks of N2 and N3, but not N1, sleep (Prerau et al., 2017; Steriade et al., 1993). In contrast to observations during natural sleep, under propofol anesthesia we observed region-specific (not global) increases in delta power (see Fig. 2b), and increases in frontal alpha power (see Fig. 2b). These observations under propofol are consistent with previous reports (Chennu et al., 2016; Ni Mhuircheartaigh et al., 2013; Pryor et al., 2004; Purdon et al., 2013; Supp et al., 2011; Tinker et al., 1977; Wang et al., 2014), and some have suggested that changes in frontal alpha and delta power are reliable indicators of loss of consciousness under propofol (Purdon et al., 2013). However, a recent study using the isolated forearm technique challenges the reliability of such an approach (Gaskell et al., 2017). Consistent with the latter findings, changes in power in the present study did not consistently distinguish N1 from N2, and S from U (see Fig. 2). In addition, these changes across arousal states were not consistently paralleled by changes in connectivity. For example, alpha power did not consistently increase in N2 compared to WS and N1 states, yet this band exhibited the most prominent connectivity changes observed during sleep (see Fig. 2, Fig. 4). Conversely, although the transition to N2 and N3 sleep was characterized by an increase in

delta power in multiple ROIs, connectivity within and across these ROIs did not undergo a comparable degree of reorganization (see Fig, 2, Supplementary Fig. 6a). These results indicate that the observed changes in connectivity do not merely follow changes in power and instead reflect functional reorganization of cortical networks. The absence of meaningful correlations between connectivity and power (see Results) further support this idea.

4.2. Changes in connectivity during sleep and anesthesia

The sharing of information between cortical regions is a critical element in theories of consciousness and brain function (Dehaene and Changeux, 2011; Friston, 2005; Tononi et al., 2016). Altered cortical connectivity observed during sleep and anesthesia has been interpreted within this theoretical context to explain reduced awareness upon LOC (Alkire et al., 2008; Mashour and Hudetz, 2017). Although there have been studies that examined functional connectivity during sleep and anesthesia (Boly et al., 2012a; Boly et al., 2012b; Lee et al., 2017; Lee et al., 2013b; Murphy et al., 2011; Ranft et al., 2016; Spoormaker et al., 2010), no previous study has directly compared the two in the same subjects. Of particular relevance is the study by Murphy et al. (2011) that examined changes in neural activity during sleep and anesthesia. However, that study utilized data from two different sets of subjects and did not compare changes in functional connectivity between the two data sets. A recent study in human volunteers that did measure changes in functional connectivity patterns derived from fMRI during transitions in arousal state found substantial differences between sleep and propofol anesthesia (again, imaged in two different groups of subjects) (Li et al., 2018). Interestingly, the latter study found that cortical changes during NREM sleep were confined to frontal cortex, while changes under propofol anesthesia were widespread. Here, measuring ECoG-derived functional connectivity in the same subjects during sleep and anesthesia, we found substantial overlap in the regional changes in functional connectivity during transitions in arousal state.

We observed consistent and pronounced changes in connectivity upon transitions into N2 and U as quantified by the difference norms and classifier analyses. What is novel about the results presented here is the degree of overlap between changes in connectivity profiles across arousal states in sleep and anesthesia. This overlap included a pronounced transition boundary between N1 and N2, and between S and U (Fig. 4). On a superficial level, one might expect some overlap in arousal states, and thus in the changes upon transitions between arousal states, during sleep and anesthesia, yet differences are expected as well. For example, WS and WA are both wake states, but disparities in the time of day of the recordings (overnight versus morning), the behavioral state of the subject (e.g. WA was just prior to major surgery), and environment (monitoring suite versus operating room) could result in substantial differences in cortical network organization. Similarly, although both N2 and U are unresponsive states with low probability of reportable conscious experience, differences in brain state due to the presence of endogenous sleep factors versus the anesthetic agent might result in distinct brain connectivity patterns. Indeed, the analysis using difference norms did not find the N2 and U connectivity profiles to be more similar to each other than to other states across the transition boundary. This is likely due to the conservative nature of the analysis, in that any differences in the connectivity between

specific ROIs will manifest in the element-by-element differences between adjacency matrices. By contrast, classification analysis did find N2 and U states to be similar, in that U data segments were easily categorized as N2-like. This is likely because the classifier analysis utilized overall patterns of connectivity rather than individual connections to categorize connectivity profiles.

Previous studies of the incidence of dreaming and conscious experience under anesthesia suggest that the observed transition boundary may reflect entry into and out of conscious states. Specifically, on one side of the boundary are states in which subjects are likely having conscious experiences, i.e. responsive (WS, WA, S) or dreaming frequently and vividly with high incidence of reportable conscious experience (REM, N1). On the other side are arousal states in which subjects are unlikely to be having conscious experiences, i.e. unresponsive (U) and with low incidence of reportable conscious experience (N2, N3) (Leslie et al., 2009; Siclari et al., 2013). This boundary was observed both with difference norms and classification analyses applied to the ROI-by-ROI adjacency matrices (see Fig. 4, 5) and with the analysis of intra-regional and long-range connectivity (see Fig. 6). However, even though connectivity patterns during propofol sedation (S) generally aligned with other conscious states, both the classification and intra-regional connectivity analyses were consistent with fluctuations in arousal level in this state (see Fig. 5b, 6a).

Two features of the changes in connectivity associated with transitions into both N2 and U were increased connectivity strength within and between anterior (frontal) brain regions, as has been observed using electrophysiological measures previously under propofol anesthesia (Purdon et al., 2013; Supp et al., 2011), and reduced connectivity elsewhere. A recent essay on the neural correlates of consciousness (NCC) suggests an interesting interpretation of these aspects of the changes in connectivity. Boly and colleagues (Boly et al., 2017) presented evidence from lesion studies and from experiments utilizing serial awakening during sleep to argue that the “full NCC”, that is the collection of all regions underlying specific contents of consciousness, comprises large portions of the parietal, occipital, and temporal lobes, whereas frontal lobe structures underlie functions associated with, but not necessary for, those conscious contents. The regions within the full NCC are most closely associated with sensory awareness, and thus would underlie the internal generative models central to theories of predictive processing and the mismatch detection and message passing functions critical to those schemes (Friston, 2005). Within this context, the focus on alpha-band connectivity is particularly relevant.

Alpha-band oscillations play a role in regulating attention and access to stored information, and intact communication in the alpha band is likely critical for sensory and semantic processing (Klimesch, 2012; Mayer et al., 2016). For example, alpha-band power and phase synchronization in particular are associated with feedback connectivity in the visual cortical hierarchy (Buffalo et al., 2011; van Kerkoerle et al., 2014). Alpha-band feedback signals have also been shown to carry predictive information in language processing (Wang et al., 2018). Changes in connectivity associated with transitions between arousal states observed in the present study are consistent with these functional roles of alpha-band oscillations. (van Kerkoerle et al., 2014). For example, it is possible that the shift in cortical connectivity from temporal to frontal lobes upon LOC may reflect a reduction in predictive processing during

states of reduced consciousness. This is consistent with the finding that anterior alpha synchronization of EEG in response to propofol correlates with disrupted sensory processing in human volunteers (Supp et al., 2011).

Although clinical considerations precluded electrode coverage of the thalamus, previous studies suggest that some of the changes in cortico-cortical connectivity observed in this study could be driven by altered thalamo-cortical synchronization (Saalmann et al., 2012). For example, the increased thalamo-cortical synchronization observed during sleep spindles (Andrillon et al., 2011) and during propofol anesthesia (Flores et al., 2017) may have a similar effect on functional connectivity within frontal cortex, as suggested by computational studies (Vijayan et al., 2013). However, the observations that the frontal shift in alpha-band connectivity was even more pronounced in N3 than it is in N2 (Supplementary Fig. 7), even though spindles are less common in N3 (Andrillon et al., 2011), and that significant changes in alpha power were not observed during sleep (see Fig. 2a), suggest that the changes in alpha-band connectivity were unlikely driven solely by sleep spindle activity.

The disintegration of cortical networks observed upon LOC during sleep, anesthesia, and coma (Alkire et al., 2008) has been ascribed to disrupted long-range connectivity. For example, several reports suggest reduced resting-state cortico-cortical (fronto-parietal) feedback connectivity under a variety of anesthetic agents, including propofol (fMRI: (Boly et al., 2012a; Ranft et al., 2016); EEG: (Lee et al., 2013b)), consistent with results using invasive electrophysiological recordings in rodent models (Imas et al., 2005; Raz et al., 2014). Disrupted long-range resting-state functional connectivity has also been reported in fMRI studies during NREM sleep (Spoormaker et al., 2010) and anesthesia (Ranft et al., 2016). However, other studies have shown no differences in changes in short- versus long-range connectivity (fMRI: Monti et al., 2013), or even increases in long-range connectivity during anesthesia (fMRI: Murphy et al., 2011; EEG: Lee et al., 2017) and sleep (fMRI: Boly et al., 2012b). Similarly, in the present study, we saw little evidence for decreases specifically in long-range connections (see Fig. 6b). The reasons for the diverse findings of the effects on connectivity are unclear. It is possible that the dynamics and heterogeneity of the resting state cortical network contribute to this diversity. For example, network configuration prior to LOC has been shown to influence observed changes in connectivity during sleep (Wilson et al., 2019). Application of methods to these data that can characterize connectivity at finer temporal resolution may address this issue.

4.3. Caveats and limitations

The key limitations of this study are the small number of participants ($n = 5$), and that the subjects had a neurologic disorder, and thus may not be entirely representative of a healthy population. These caveats are inherent to all human intracranial electrophysiology studies. Our statistical methods focused on within-subject comparisons between states and should be generalized with caution. However, results were consistent across subjects who all had different clinical histories of their seizure disorder, antiepileptic medication regimens, and seizure foci. Recordings from cortical sites confirmed to be seizure foci were excluded from analyses. Finally, all subjects participated in multiple additional research protocols over the course of their hospitalization, including a range of behavioral tasks. Behavioral and neural

data obtained in these other experiments were examined for consistency with a corpus of published human intracranial electrophysiology data (reviewed in (Nourski, 2017). None of the subjects exhibited aberrant responses that could be interpreted as grounds for caution in inclusion in this study.

Caveats that are specific to this study include possible effects of seizures, AED use, and hospital environment on sleep and anesthesia. Seizures can have acute disruptive effects on sleep architecture (Derry and Duncan, 2013; Jain and Kothare, 2015; Touchon et al., 1991). In the present study, subjects were monitored for seizure activity during the overnight sleep recording to avoid acute effects of seizures on sleep. In the one subject who had overnight seizures (L403), data that were collected after seizures commenced were excluded from analysis. Additionally, chronic use of AEDs can affect the quality and structure of sleep (Jain and Glauser, 2014). In the present study, overnight sleep data were collected when the subjects were weaned off their AEDs as part of their clinical seizure monitoring protocol. This reduced any effects of the AED use on the quality of sleep data in our subject cohort. It should be noted that sleep stage scoring was independent of these confounding factors, and all subjects had sufficient duration of each stage of sleep (REM, N1, N2) for the purposes of analysis presented here. The hospital environment may also have had an impact on the quality and structure of overnight sleep in the studied subjects. This may have contributed to the lack of observed N3 sleep stage in two out of five subjects. Finally, the use of AEDs can lead to a reduction of the dose of propofol required to achieve surgical level of general anesthesia (Ouchi and Sugiyama, 2015). However, estimated plasma propofol concentrations at loss of responsiveness in the present subject cohort (2.31 μg/ml on average) are comparable to those reported in literature (Doufas et al., 2001; Iwakiri et al., 2005; Li et al., 2018). In addition, the present study did not depend on specific dose of propofol but rather on behavioral assessment of arousal. Thus, overall the definition of arousal states that was central to the analysis was not affected by the confounding factors secondary to the subjects' history of epilepsy, allowing us to measure brain states regardless of them. All of these factors may have contributed to variability in connectivity measures, making detection of differences across arousal states more difficult. This makes the positive findings of the current study all the more striking.

The motivation for exploring changes in connectivity across arousal states is to elucidate the neural underpinnings that define these states. We note, however, that the arousal states as defined in this study are likely non-uniform regarding consciousness. For example, healthy adults are able to report on conscious experience (i.e. dreaming) about 40% and 20% of the time in N2 and N3 sleep (Siclari et al., 2013). Dreaming also occurs under propofol anesthesia in about 20% of patients (Leslie et al., 2009). This suggests that differences in brain connectivity between the conscious and unconscious states may be even greater than those reported here, had it been possible to distinguish reliably dreaming vs. non-dreaming states in our data set.

We also note the challenges in assessing awareness under anesthesia, and specifically the delicate balance between interrogating a subject's awareness and changing the state of their arousal with that interrogation. The approach employed here, the OAA/S, is considered the gold standard for assessing awareness in the perioperative setting (Chernik et al., 1990), and

it has been cross-validated using EEG-based measures such as BIS (Vanluchene et al., 2004). The BIS values recorded in the current study corresponded well to those associated with wake, sedated, and unconscious states in previous reports (Vanluchene et al., 2004). Importantly, we did not observe consistent increases in BIS values post-OAA/S assessments compared to pre-OAA/S assessments (see Supplementary Fig. 2), indicating that our assessments likely did not alter the arousal state of the subjects.

4.4. Functional significance and future directions

The results presented here have broad implications for understanding the neural mechanisms associated with loss of consciousness and for better understanding and differential diagnosis of disorders of consciousness. We demonstrate a transition boundary in profiles of functional connectivity that separates states of different levels of consciousness. Phase synchronization is postulated to mediate rapid communication of conscious content over multiple spatial scales in cortex, contributing importantly to the rich repertoire of human behavior that characterizes conscious states (Fries, 2015). The finding that changes in functional connectivity based on phase synchronization indexes arousal state similarly in both sleep and anesthesia motivates further exploration of the changes in brain activity and connectivity common to changes in consciousness. These findings have practical clinical ramifications as well. Connectivity can be measured non-invasively using EEG or fMRI in patients with disorders of consciousness. Algorithms that track region-specific functional connectivity may provide a basis for noninvasive monitoring of arousal state in patients otherwise inaccessible to standard assessments of arousal based on response to command. Future experiments aimed at exploring in more detail the differences between LOC in sleep and anesthesia, and generalizing to other anesthetic agents such as dexmedetomidine and volatile anesthetics, will elucidate further fundamental questions about the nature of consciousness and arousal that remain unresolved.

Supplementary Material

Refer to Web version on PubMed Central for supplementary material.

Acknowledgements

This work was supported by the National Institutes of Health (grant numbers R01-DC04290, R01-GM109086, UL1-RR024979). We are grateful to Jess Banks, Haiming Chen, Phillip Gander, Christine Glenn, Bradley Hindman, Matthew Howard, Richard Lennertz, Rashmi Mueller, Ariane Rhone, Robert Sanders, Beau Snoad, Mitchell Steinschneider, Deanne Tadlock, and Thoru Yamada for help with data collection, analysis, and comments on the manuscript.

REFERENCES CITED

Akeju O, Brown EN, 2017 Neural oscillations demonstrate that general anesthesia and sedative states are neurophysiologically distinct from sleep. Curr Opin Neurobiol 44, 178–185. [PubMed: 28544930]

Alkire MT, Hudetz AG, Tononi G, 2008 Consciousness and anesthesia. Science 322, 876–880. [PubMed: 18988836]

Andrillon T, Nir Y, Staba RJ, Ferrarelli F, Cirelli C, Tononi G, Fried I, 2011 Sleep spindles in humans: insights from intracranial EEG and unit recordings. J Neurosci 31, 17821–17834. [PubMed: 22159098]

Bates D, Mächler M, Bolker B, Walker S, 2015 Fitting Linear Mixed-Effects Models Using lme4. J Stat Software 67, 48.

Bayne T, Hohwy J, Owen AM, 2017 Reforming the taxonomy in disorders of consciousness. Ann Neurol 82, 866–872. [PubMed: 29091304]

Bernat JL, 2017 Nosologic considerations in disorders of consciousness. Ann Neurol 82, 863–865. [PubMed: 29092102]

Berry RB, Brooks R, Gamaldo CE, Harding SM, Lloyd RM, Marcus CL, Vaughn BV, Medicine, f.t.A.A.o.S., 2017 AASM Manual for the Scoring of Sleep and Associated Events: Rules, Terminology and Technical Specifications, Version 2.4, 1 ed. American Academy of Sleep Medicine, Darien, IL.

Besag J, Clifford P, 1989 Generalized Monte-Carlo Significance Tests. Biometrika 76, 633–642.

Blain-Moraes S, Lee U, Ku S, Noh G, Mashour GA, 2014 Electroencephalographic effects of ketamine on power, cross-frequency coupling, and connectivity in the alpha bandwidth. Front Syst Neurosci 8, 114. [PubMed: 25071473]

Blain-Moraes S, Tarnal V, Vanini G, Alexander A, Rosen D, Shortal B, Janke E, Mashour GA, 2015 Neurophysiological correlates of sevoflurane-induced unconsciousness. Anesthesiology 122, 307–316. [PubMed: 25296108]

Boly M, Massimini M, Tsuchiya N, Postle BR, Koch C, Tononi G, 2017 Are the Neural Correlates of Consciousness in the Front or in the Back of the Cerebral Cortex? Clinical and Neuroimaging Evidence. J Neurosci 37, 9603–9613. [PubMed: 28978697]

Boly M, Moran R, Murphy M, Boveroux P, Bruno MA, Noirhomme Q, Ledoux D, Bonhomme V, Brichant JF, Tononi G, Laureys S, Friston K, 2012a Connectivity changes underlying spectral EEG changes during propofol-induced loss of consciousness. J Neurosci 32, 7082–7090. [PubMed: 22593076]

Boly M, Perlbarg V, Marrelec G, Schabus M, Laureys S, Doyon J, Pelegrini-Issac M, Maquet P, Benali H, 2012b Hierarchical clustering of brain activity during human nonrapid eye movement sleep. Proc Natl Acad Sci USA 109, 5856–5861. [PubMed: 22451917]

Brugge JF, Nourski KV, Oya H, Reale RA, Kawasaki H, Steinschneider M, Howard MA 3rd, 2009 Coding of repetitive transients by auditory cortex on Heschl's gyrus. J Neurophysiol 102, 2358–2374. [PubMed: 19675285]

Buffalo EA, Fries P, Landman R, Buschman TJ, Desimone R, 2011 Laminar differences in gamma and alpha coherence in the ventral stream. Proceedings of the National Academy of Sciences 108, 11262–11267.

Chennu S, O'Connor S, Adapa R, Menon DK, Bekinschtein TA, 2016 Brain Connectivity Dissociates Responsiveness from Drug Exposure during Propofol-Induced Transitions of Consciousness. PLOS Comput Biol 12, e1004669. [PubMed: 26764466]

Chernik DA, Gillings D, Laine H, Hendler J, Silver JM, Davidson AB, Schwam EM, Siegel JL, 1990 Validity and reliability of the Observer's Assessment of Alertness/Sedation Scale: study with intravenous midazolam. J Clin Psychopharmacol 10, 244–251. [PubMed: 2286697]

Cliff N, 1993 Dominance Statistics - Ordinal Analyses to Answer Ordinal Questions. Psychological Bulletin 114, 494–509.

Dehaene S, Changeux JP, 2011 Experimental and theoretical approaches to conscious processing. Neuron 70, 200–227. [PubMed: 21521609]

Derry CP, Duncan S, 2013 Sleep and epilepsy. Epilepsy Behav 26, 394–404. [PubMed: 23465654]

Destrieux C, Fischl B, Dale A, Halgren E, 2010 Automatic parcellation of human cortical gyri and sulci using standard anatomical nomenclature. Neuroimage 53, 1–15. [PubMed: 20547229]

Destrieux C, Terrier LM, Andersson F, Love SA, Cottier JP, Duvernoy H, Velut S, Janot K, Zemmoura I, 2017 A practical guide for the identification of major sulcogyral structures of the human cortex. Brain Struct Funct 222, 2001–2015. [PubMed: 27709299]

Doufas AG, Bakhshandeh M, Bjorksten AR, Greif R, Sessler DI, 2001 Automated responsiveness test (ART) predicts loss of consciousness and adverse physiologic responses during propofol conscious sedation. Anesthesiology 94, 585–592. [PubMed: 11379677]

Drummond JC, 2000 Monitoring depth of anesthesia: with emphasis on the application of the bispectral index and the middle latency auditory evoked response to the prevention of recall. Anesthesiology 93, 876–882. [PubMed: 10969323]

Eer AS, Padmanabhan U, Leslie K, 2009 Propofol dose and incidence of dreaming during sedation. Eur J Anaesthesiol 26, 833–836. [PubMed: 19528807]

Flores FJ, Hartnack KE, Fath AB, Kim SE, Wilson MA, Brown EN, Purdon PL, 2017 Thalamocortical synchronization during induction and emergence from propofol-induced unconsciousness. Proc Natl Acad Sci U S A 114, E6660–E6668. [PubMed: 28743752]

Fries P, 2015 Rhythms for Cognition: Communication through Coherence. Neuron 88, 220–235. [PubMed: 26447583]

Friston K, 2005 A theory of cortical responses. Philos Trans R Soc Lond B Biol Sci 360, 815–836. [PubMed: 15937014]

Gan TJ, Glass PS, Windsor A, Payne F, Rosow C, Sebel P, Manberg P, 1997 Bispectral index monitoring allows faster emergence and improved recovery from propofol, alfentanil, and nitrous oxide anesthesia. BIS Utility Study Group. Anesthesiology 87, 808–815. [PubMed: 9357882]

Gaskell AL, Hight DF, Winders J, Tran G, Defresne A, Bonhomme V, Raz A, Sleigh JW, Sanders RD, 2017 Frontal alpha-delta EEG does not preclude volitional response during anaesthesia: prospective cohort study of the isolated forearm technique. Br J Anaesth 119, 664–673. [PubMed: 29121278]

Glass PS, Bloom M, Kearse L, Rosow C, Sebel P, Manberg P, 1997 Bispectral analysis measures sedation and memory effects of propofol, midazolam, isoflurane, and alfentanil in healthy volunteers. Anesthesiology 86, 836–847. [PubMed: 9105228]

Heard NA, Rubin-Delanchy P, 2018 Choosing between methods of combining p-values. Biometrika 105, 239–246.

Imas OA, Ropella KM, Ward BD, Wood JD, Hudetz AG, 2005 Volatile anesthetics disrupt frontal-posterior recurrent information transfer at gamma frequencies in rat. Neurosci.Lett 387, 145–150. [PubMed: 16019145]

Iwakiri H, Nishihara N, Nagata O, Matsukawa T, Ozaki M, Sessler DI, 2005 Individual effect-site concentrations of propofol are similar at loss of consciousness and at awakening. Anesth Analg 100, 107–110. [PubMed: 15616062]

Jain SV, Glauser TA, 2014 Effects of epilepsy treatments on sleep architecture and daytime sleepiness: an evidence-based review of objective sleep metrics. Epilepsia 55, 26–37. [PubMed: 24299283]

Jain SV, Kothare SV, 2015 Sleep and Epilepsy. Semin Pediatr Neurol 22, 86–92. [PubMed: 26072338]

Jenkinson M, Bannister P, Brady M, Smith S, 2002 Improved optimization for the robust and accurate linear registration and motion correction of brain images. Neuroimage 17, 825–841. [PubMed: 12377157]

Klimesch W, 2012 alpha-band oscillations, attention, and controlled access to stored information. Trends Cogn Sci 16, 606–617. [PubMed: 23141428]

Kovach CK, Gander PE, 2016 The demodulated band transform. J Neurosci Methods 261, 135–154. [PubMed: 26711370]

Kremen V, Brinkmann BH, Van Gompel JJ, Stead M, St Louis EK, Worrell GA, 2019 Automated unsupervised behavioral state classification using intracranial electrophysiology. J Neural Eng 16, 026004. [PubMed: 30277223]

Lee H, Mashour GA, Noh GJ, Kim S, Lee U, 2013a Reconfiguration of network hub structure after propofol-induced unconsciousness. Anesthesiology 119, 1347–1359. [PubMed: 24013572]

Lee M, Sanders RD, Yeom SK, Won DO, Seo KS, Kim HJ, Tononi G, Lee SW, 2017 Network Properties in Transitions of Consciousness during Propofol-induced Sedation. Sci Rep 7, 16791. [PubMed: 29196672]

Lee U, Ku S, Noh G, Baek S, Choi B, Mashour GA, 2013b Disruption of frontal-parietal communication by ketamine, propofol, and sevoflurane. Anesthesiology 118, 1264–1275. [PubMed: 23695090]

Lenth RV, 2019 emmeans: Estimated Marginal Means, aka Least-Squares Means. R package version 1.3.3.

Leslie K, Sleigh J, Paech MJ, Voss L, Lim CW, Sleigh C, 2009 Dreaming and electroencephalographic changes during anesthesia maintained with propofol or desflurane. Anesthesiology 111, 547–555. [PubMed: 19672164]

Li Y, Wang S, Pan C, Xue F, Xian J, Huang Y, Wang X, Li T, He H, 2018 Comparison of NREM sleep and intravenous sedation through local information processing and whole brain network to explore the mechanism of general anesthesia. PLoS One 13, e0192358. [PubMed: 29486001]

Liu X, Lauer KK, Ward BD, Rao SM, Li SJ, Hudetz AG, 2012 Propofol disrupts functional interactions between sensory and high-order processing of auditory verbal memory. Hum Brain Mapp 33, 2487–2498. [PubMed: 21932265]

Lydic R, Baghdoyan HA, 2005 Sleep, anesthesiology, and the neurobiology of arousal state control. Anesthesiology 103, 1268–1295. [PubMed: 16306742]

MacIver MB, Bland BH, 2014 Chaos analysis of EEG during isoflurane-induced loss of righting in rats. Front Syst Neurosci 8, 203. [PubMed: 25360091]

Mashour G, 2020 Assessing the Anesthetized State with the Electroencephalogram. pp. 43–47.

Mashour GA, 2006 Integrating the science of consciousness and anesthesia. Anesth Analg. 103, 975–982. [PubMed: 17000815]

Mashour GA, Hudetz AG, 2017 Bottom-Up and Top-Down Mechanisms of General Anesthetics Modulate Different Dimensions of Consciousness. Front Neural Circuits 11, 44. [PubMed: 28676745]

Mayer A, Schwiedrzik CM, Wibral M, Singer W, Melloni L, 2016 Expecting to See a Letter: Alpha Oscillations as Carriers of Top-Down Sensory Predictions. Cereb Cortex 26, 3146–3160. [PubMed: 26142463]

Monti MM, Lutkenhoff ES, Rubinov M, Boveroux P, Vanhaudenhuyse A, Gosseries O, Bruno MA, Noirhomme Q, Boly M, Laureys S, 2013 Dynamic change of global and local information processing in propofol-induced loss and recovery of consciousness. PLOS Comput Biol 9, e1003271. [PubMed: 24146606]

Murphy M, Bruno MA, Riedner BA, Boveroux P, Noirhomme Q, Landsness EC, Brichant JF, Phillips C, Massimini M, Laureys S, Tononi G, Boly M, 2011 Propofol anesthesia and sleep: a high-density EEG study. Sleep 34, 283–291A. [PubMed: 21358845]

Nagahama Y, Kovach CK, Ciliberto M, Joshi C, Rhone AE, Vesole A, Gander PE, Nourski KV, Oya H, Howard MA 3rd, Kawasaki H, Dlouhy BJ, 2018 Localization of musicogenic epilepsy to Heschl's gyrus and superior temporal plane: case report. J Neurosurg 129, 157–164. [PubMed: 28946181]

Ni Mhuircheartaigh R, Warnaby C, Rogers R, Jbabdi S, Tracey I, 2013 Slow-wave activity saturation and thalamocortical isolation during propofol anesthesia in humans. Sci Transl Med 5, 208ra148.

Nir Y, Vyazovskiy VV, Cirelli C, Banks MI, Tononi G, 2015 Auditory responses and stimulus-specific adaptation in rat auditory cortex are preserved across NREM and REM sleep. Cereb Cortex 25, 1362–1378. [PubMed: 24323498]

Nourski KV, 2017 Auditory processing in the human cortex: An intracranial electrophysiology perspective. Laryngoscope Investig Otolaryngol 2, 147–156.

Nourski KV, Howard MA 3rd, 2015 Invasive recordings in the human auditory cortex. Handb Clin Neurol 129, 225–244. [PubMed: 25726272]

Nourski KV, Steinschneider M, Rhone AE, 2016 Electrocorticographic Activation within Human Auditory Cortex during Dialog-Based Language and Cognitive Testing. Front Hum Neurosci 10, 202. [PubMed: 27199720]

Nourski KV, Steinschneider M, Rhone AE, Kawasaki H, Howard MA 3rd, Banks MI, 2018a Auditory Predictive Coding across Awareness States under Anesthesia: An Intracranial Electrophysiology Study. J Neurosci 38, 8441–8452. [PubMed: 30126970]

Nourski KV, Steinschneider M, Rhone AE, Kawasaki H, Howard MA 3rd, Banks MI, 2018b Processing of auditory novelty across the cortical hierarchy: An intracranial electrophysiology study. Neuroimage 183, 412–424. [PubMed: 30114466]

Otto KA, 2008 EEG power spectrum analysis for monitoring depth of anaesthesia during experimental surgery. Lab Anim 42, 45–61. [PubMed: 18348766]

Ouchi K, Sugiyama K, 2015 Required propofol dose for anesthesia and time to emerge are affected by the use of antiepileptics: prospective cohort study. BMC Anesthesiol 15, 34. [PubMed: 25788855]

Prerau MJ, Brown RE, Bianchi MT, Ellenbogen JM, Purdon PL, 2017 Sleep Neurophysiological Dynamics Through the Lens of Multitaper Spectral Analysis. Physiology (Bethesda) 32, 60–92. [PubMed: 27927806]

Pryor KO, Veselis RA, Reinsel RA, Feshchenko VA, 2004 Enhanced visual memory effect for negative versus positive emotional content is potentiated at sub-anaesthetic concentrations of thiopental. Br.J Anaesth 93, 348–355. [PubMed: 15220170]

Purdon PL, Pierce ET, Mukamel EA, Prerau MJ, Walsh JL, Wong KF, Salazar-Gomez AF, Harrell PG, Sampson AL, Cimenser A, Ching S, Kopell NJ, Tavares-Stoeckel C, Habeeb K, Merhar R, Brown EN, 2013 Electroencephalogram signatures of loss and recovery of consciousness from propofol. Proc Natl Acad Sci U S A 110, E1142–1151. [PubMed: 23487781]

Ranft A, Golkowski D, Kiel T, Riedl V, Kohl P, Rohrer G, Pientka J, Berger S, Thul A, Maurer M, Preibisch C, Zimmer C, Mashour GA, Kochs EF, Jordan D, Ilg R, 2016 Neural Correlates of Sevoflurane-induced Unconsciousness Identified by Simultaneous Functional Magnetic Resonance Imaging and Electroencephalography. Anesthesiology 125, 861–872. [PubMed: 27617689]

Raz A, Grady SM, Krause BM, Uhlrich DJ, Manning KA, Banks MI, 2014 Preferential effect of isoflurane on top-down versus bottom-up pathways in sensory cortex. Front Syst Neurosci 8.

Reddy CG, Dahdaleh NS, Albert G, Chen F, Hansen D, Nourski K, Kawasaki H, Oya H, Howard MA 3rd, 2010 A method for placing Heschl gyrus depth electrodes. J Neurosurg 112, 1301–1307. [PubMed: 19663547]

Rohr K, Stiehl HS, Sprengel R, Buzug TM, Weese J, Kuhn MH, 2001 Landmark-based elastic registration using approximating thin-plate splines. IEEE Trans Med Imaging 20, 526–534. [PubMed: 11437112]

Saalmann YB, Pinsk MA, Wang L, Li X, Kastner S, 2012 The pulvinar regulates information transmission between cortical areas based on attention demands. Science 337, 753–756. [PubMed: 22879517]

Sanders RD, Banks MI, Darracq M, Moran R, Sleigh J, Gosseries O, Bonhomme V, Brichant JF, Rosanova M, Raz A, Tononi G, Massimini M, Laureys S, Boly M, 2018 Propofol-induced unresponsiveness is associated with impaired feedforward connectivity in cortical hierarchy. Br J Anaesth 121, 1084–1096. [PubMed: 30336853]

Schnider TW, Minto CF, Gambus PL, Andresen C, Goodale DB, Shafer SL, Youngs EJ, 1998 The influence of method of administration and covariates on the pharmacokinetics of propofol in adult volunteers. Anesthesiology 88, 1170–1182. [PubMed: 9605675]

Shushruth S, 2013 Exploring the Neural Basis of Consciousness through Anesthesia. J Neurosci 33, 1757–1758. [PubMed: 23365215]

Siclari F, Larocque JJ, Postle BR, Tononi G, 2013 Assessing sleep consciousness within subjects using a serial awakening paradigm. Front Psychol 4, 542. [PubMed: 23970876]

Spoormaker VI, Schroter MS, Gleiser PM, Andrade KC, Dresler M, Wehrle R, Samann PG, Czisch M, 2010 Development of a large-scale functional brain network during human non-rapid eye movement sleep. J Neurosci 30, 11379–11387. [PubMed: 20739559]

Stein EJ, Glick DB, 2016 Advances in awareness monitoring technologies. Curr Opin Anaesthesiol 29, 711–716. [PubMed: 27585361]

Steriade M, McCormick DA, Sejnowski TJ, 1993 Thalamocortical oscillations in the sleeping and aroused brain. Science 262, 679–685. [PubMed: 8235588]

Stouffer SA, Suchman EA, DeVinney LC, Star SA, Williams RM, 1949 The American Soldier Adjustment During Army LIfe. Princeton University Press, Princeton.

Strauss M, Sitt JD, King JR, Elbaz M, Azizi L, Buiatti M, Naccache L, van Wassenhove V, Dehaene S, 2015 Disruption of hierarchical predictive coding during sleep. Proc Natl Acad Sci U S A 112, E1353–1362. [PubMed: 25737555]

Struys M, Versichelen L, Mortier E, Ryckaert D, De Mey JC, De Deyne C, Rolly G, 1998 Comparison of spontaneous frontal EMG, EEG power spectrum and bispectral index to monitor propofol drug effect and emergence. Acta Anaesthesiol Scand 42, 628–636. [PubMed: 9689266]

Supp GG, Siegel M, Hipp JF, Engel AK, 2011 Cortical hypersynchrony predicts breakdown of sensory processing during loss of consciousness. Curr Biol 21, 1988–1993. [PubMed: 22100063]

Tinker JH, Sharbrough FW, Michenfelder JD, 1977 Anterior shift of the dominant EEG rhytham during anesthesia in the Java monkey: correlation with anesthetic potency. Anesthesiology 46, 252–259. [PubMed: 402870]

Tononi G, Boly M, Massimini M, Koch C, 2016 Integrated information theory: from consciousness to its physical substrate. Nat Rev Neurosci 17, 450–461. [PubMed: 27225071]

Touchon J, Baldy-Moulinier M, Billiard M, Besset A, Cadilhac J, 1991 Sleep organization and epilepsy. Epilepsy Res Suppl 2, 73–81. [PubMed: 1760099]

Tung A, Mendelson WB, 2004 Anesthesia and sleep. Sleep Medicine Reviews 8, 213–225. [PubMed: 15144963]

van Dellen E, van der Kooi AW, Numan T, Koek HL, Klijn FA, Buijsrogge MP, Stam CJ, Slooter AJ, 2014 Decreased functional connectivity and disturbed directionality of information flow in the electroencephalography of intensive care unit patients with delirium after cardiac surgery. Anesthesiology 121, 328–335. [PubMed: 24901239]

van Kerkoerle T, Self MW, Dagnino B, Gariel-Mathis MA, Poort J, van der Togt C, Roelfsema PR, 2014 Alpha and gamma oscillations characterize feedback and feedforward processing in monkey visual cortex. Proc Natl Acad Sci U S A 111, 14332–14341. [PubMed: 25205811]

Vanluchene AL, Struys MM, Heyse BE, Mortier EP, 2004 Spectral entropy measurement of patient responsiveness during propofol and remifentanil. A comparison with the bispectral index. Br J Anaesth 93, 645–654. [PubMed: 15321934]

Vijayan S, Ching S, Purdon PL, Brown EN, Kopell NJ, 2013 Thalamocortical mechanisms for the anteriorization of alpha rhythms during propofol-induced unconsciousness. J Neurosci 33, 11070–11075. [PubMed: 23825412]

Vinck M, Oostenveld R, van Wingerden M, Battaglia F, Pennartz CM, 2011 An improved index of phase-synchronization for electrophysiological data in the presence of volume-conduction, noise and sample-size bias. Neuroimage 55, 1548–1565. [PubMed: 21276857]

Voss LJ, Garcia PS, Hentschke H, Banks MI, 2019 Understanding the Effects of General Anesthetics on Cortical Network Activity Using Ex Vivo Preparations. Anesthesiology.

Wang K, Steyn-Ross ML, Steyn-Ross DA, Wilson MT, Sleigh JW, 2014 EEG slow-wave coherence changes in propofol-induced general anesthesia: experiment and theory. Front Syst Neurosci 8, 215. [PubMed: 25400558]

Wang L, Hagoort P, Jensen O, 2018 Language Prediction Is Reflected by Coupling between Frontal Gamma and Posterior Alpha Oscillations. J Cogn Neurosci 30, 432–447. [PubMed: 28949823]

Wilf M, Ramot M, Furman-Haran E, Arzi A, Levkovitz Y, Malach R, 2016 Diminished Auditory Responses during NREM Sleep Correlate with the Hierarchy of Language Processing. PLoS One 11, e0157143. [PubMed: 27310812]

Wilson RS, Mayhew SD, Rollings DT, Goldstone A, Hale JR, Bagshaw AP, 2019 Objective and subjective measures of prior sleep-wake behavior predict functional connectivity in the default mode network during NREM sleep. Brain Behav 9, e01172. [PubMed: 30516035]

Winkler AM, Webster MA, Vidaurre D, Nichols TE, Smith SM, 2015 Multi-level block permutation. Neuroimage 123, 253–268. [PubMed: 26074200]

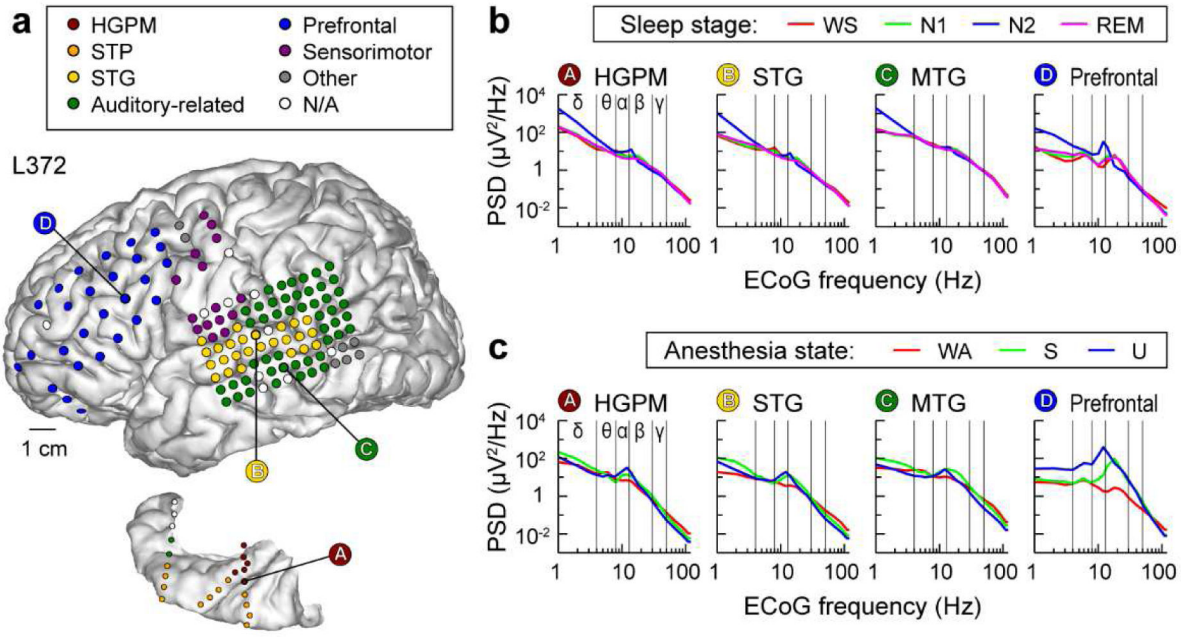

Fig. 1: Electrode coverage and electrocorticographic (ECoG) power spectra.

Exemplary data from subject L372. **a,** Electrode coverage of the lateral surface of the left cerebral hemisphere (top) and left superior temporal plane (bottom). Recording sites are color-coded according to the region of interest group (see Methods for details and Supplementary Table 3 for abbreviation key). **b,** ECoG power spectra during sleep. Data from four representative sites (left-to-right). WS: wake (sleep experiment); PSD: power spectral density. **c,** ECoG power spectra during anesthesia. WA: wake (anesthesia experiment); S: sedated; U: unresponsive.

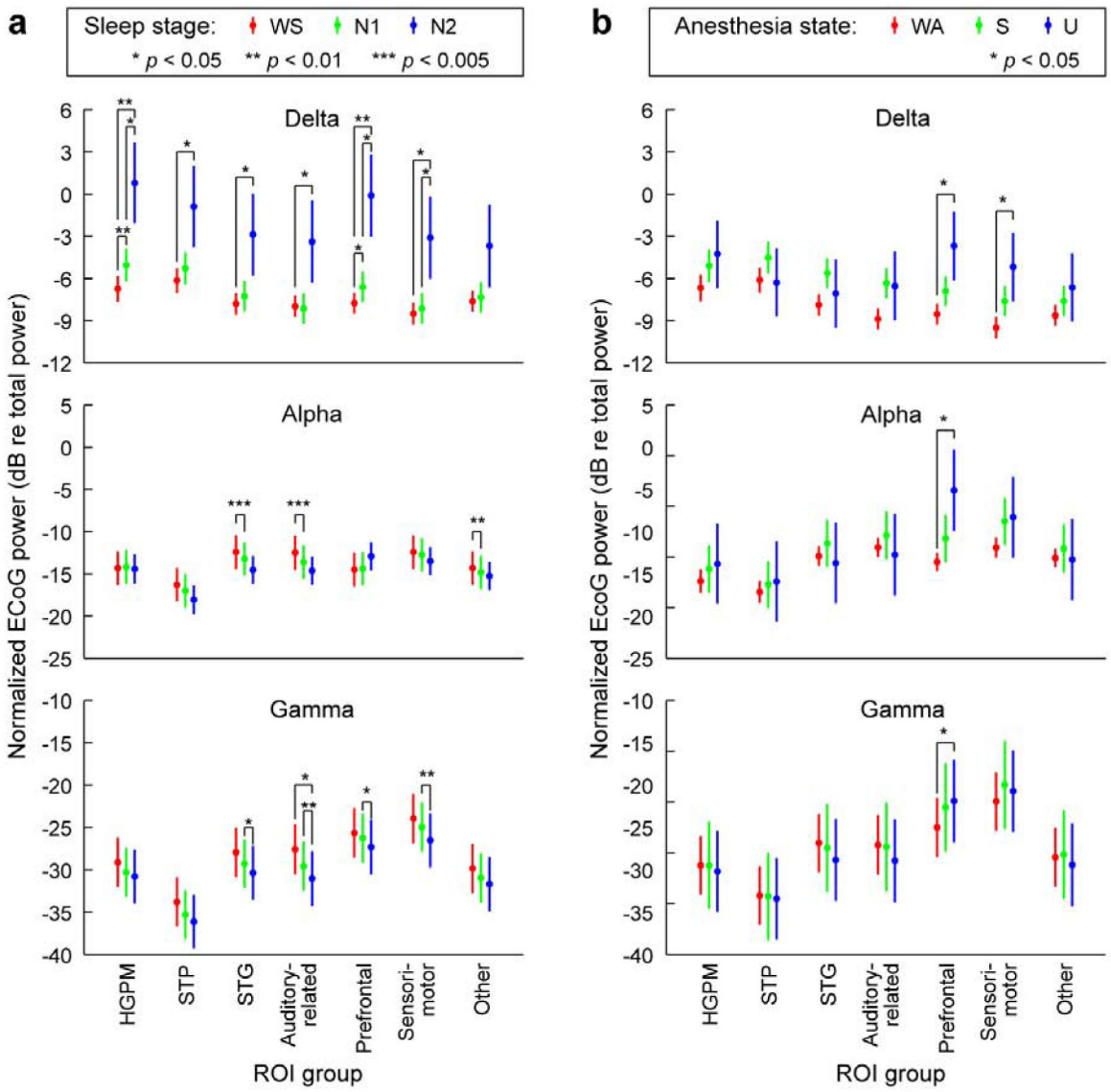

Fig. 2: Changes in ECoG band power across arousal states.

a, ECoG band power during sleep, plotted as marginal means and 95% confidence intervals. **b,** ECoG band power during anesthesia. Data from 5 subjects. Changes in delta, alpha, and gamma power are shown in top, middle and bottom rows, respectively. See Table 1 for definition of each region of interest (ROI) group. *P*-values were adjusted for multiple comparisons as described in Methods. WS: wake (sleep experiment), WA: wake (anesthesia experiment); S: sedated; U: unresponsive.

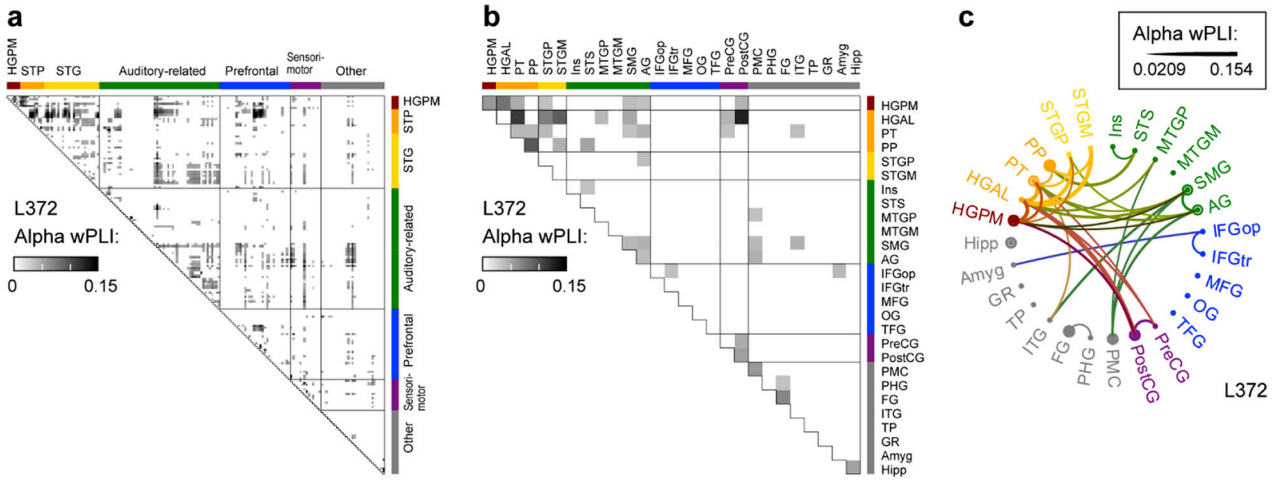

Fig. 3: Analysis of alpha-band functional connectivity in wake state.

Example from subject L372. **a,** Adjacency matrix for all recording sites. **b**, Adjacency matrix, collapsed for all regions of interest (ROIs). **c**, Chord connectivity plot. Line thickness reflects mean wPLI values that characterize pairs of ROIs. For display purposes, the chord plot was thresholded to retain the 10% strongest connections.

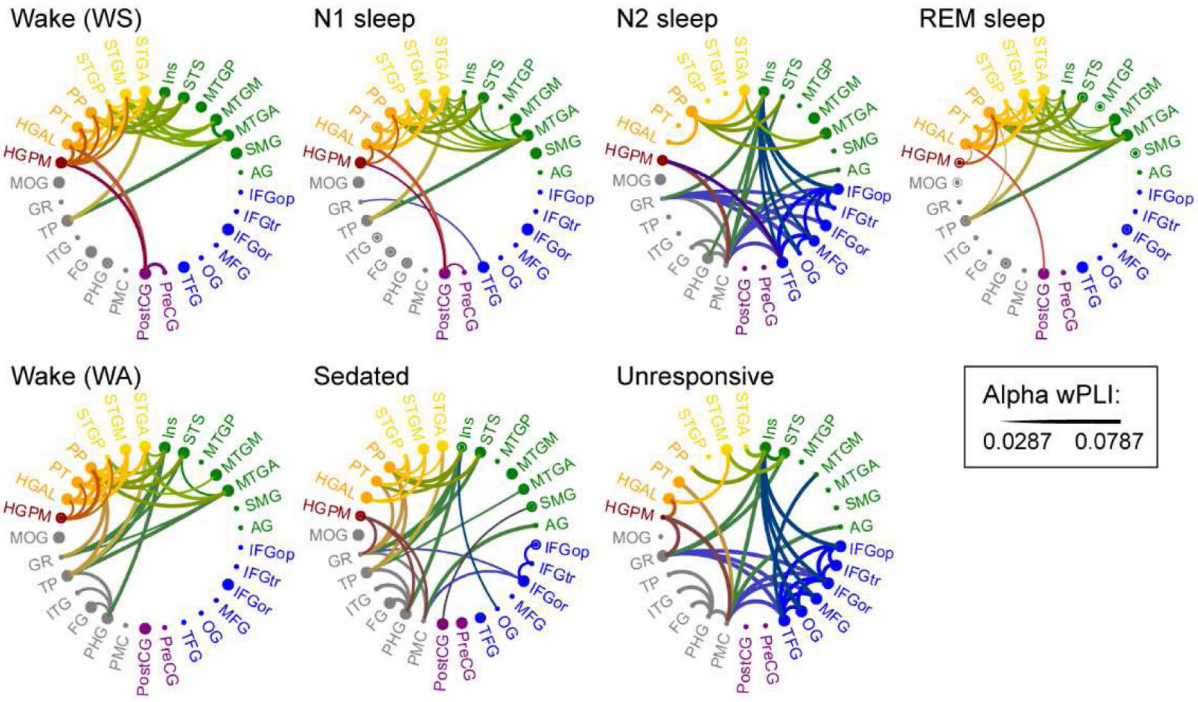

Fig. 4: ROI-based analysis of alpha-band functional connectivity across arousal states.
Data from five subjects. See caption of Fig. 3c for details.

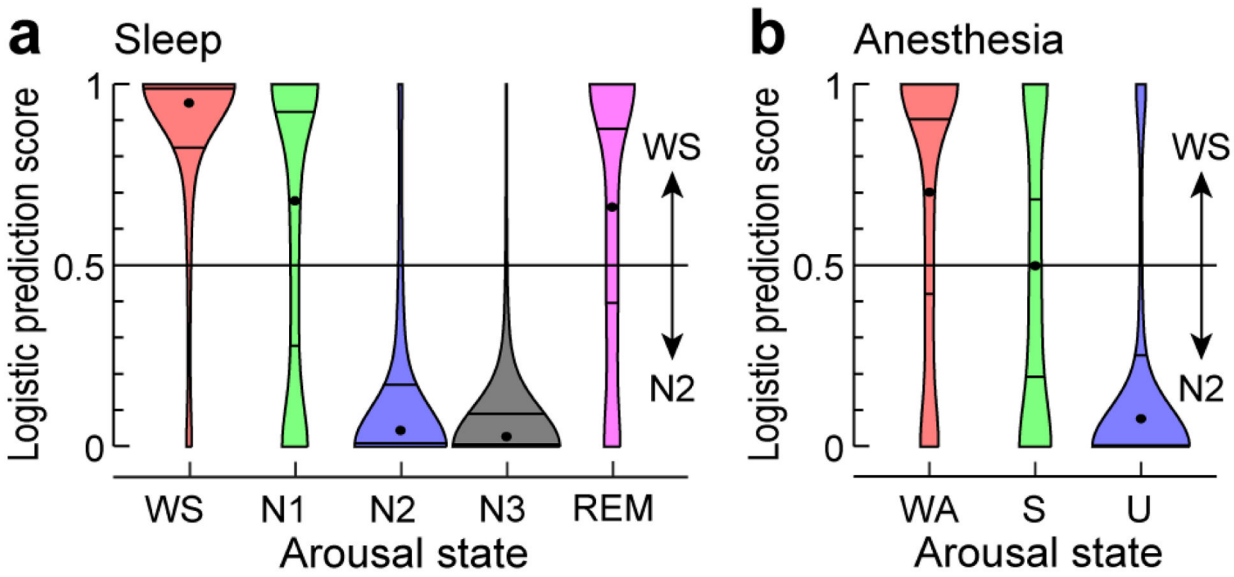

Fig. 5: Classification of data segments.

Logistic prediction distributions for adjacency matrices from sleep and anesthesia arousal states (panels **a** and **b**, respectively) analyzed by a linear classifier trained on a subset of WS and N2 data. Each violin plot shows the average distribution across five subjects (except for N3, which is for 3 subjects). Centered dot and surrounding horizontal lines represent each distribution's median, first and third quartiles, respectively. For distributions from individual subjects, see Supplementary Figure 8.

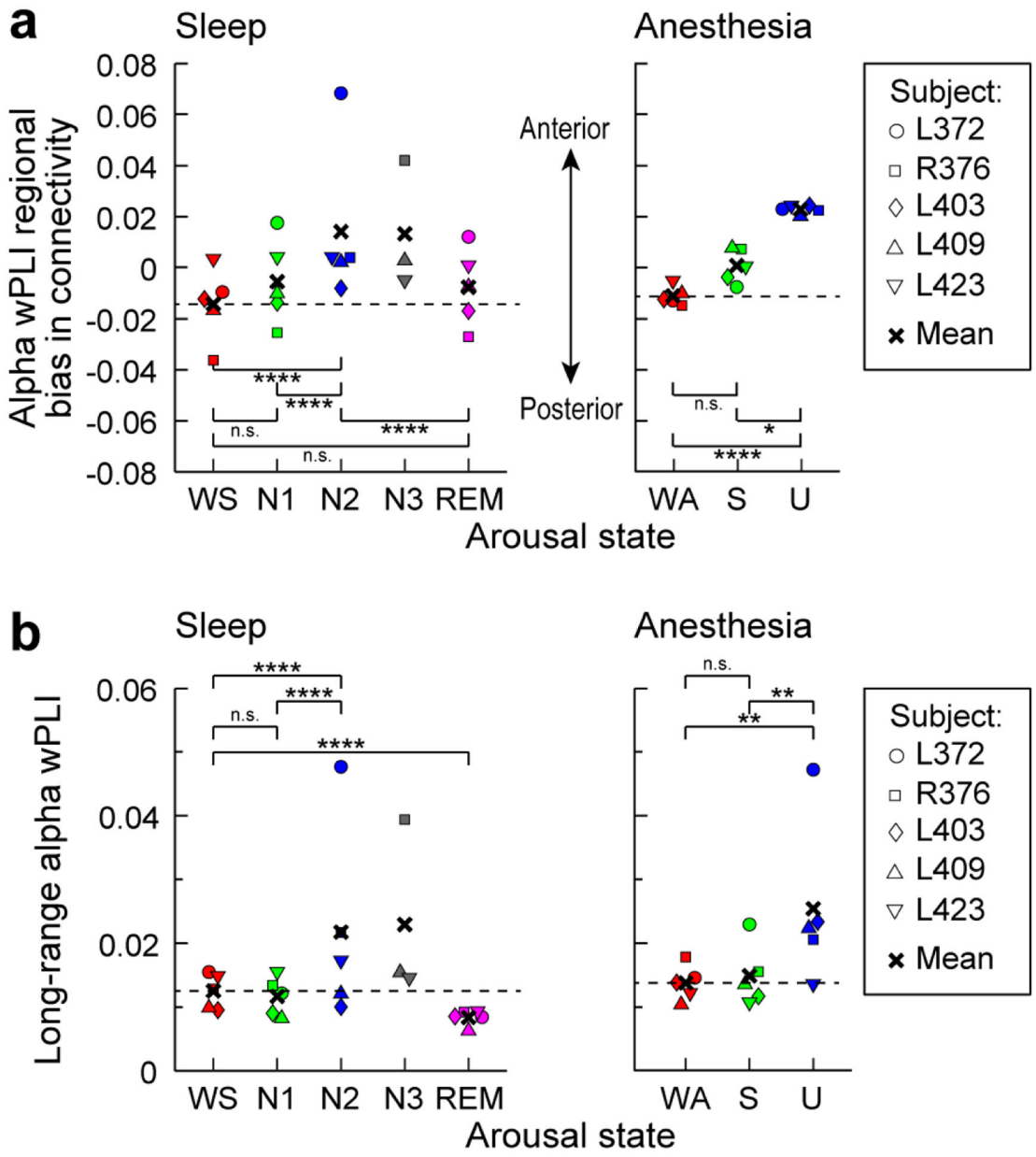

Fig. 6: Intra-regional and long-range connectivity changes with arousal state.

a: Mean alpha wPLI averaged within anterior quadrants of the adjacency matrices minus the average within posterior quadrants. Values greater than zero indicate greater within-anterior connectivity compared to within-posterior connectivity. **b:** Mean alpha wPLI values for recording site pairs distanced greater than the 75th percentile. Significance: n.s., $p > 0.05$; **, $p < 0.01$; ***, $p < 0.005$; ****, $p < 0.001$ (permutation test). Although subject L372 exhibited larger effects than the others in N2 for both analyses, and in U for the long-range connectivity analysis, statistical significance and conclusions were robust to omitting that subject's (or any individual subject's) data from the analyses. Dashed lines in **a** and **b** depict mean values during the WS and WA states for sleep and anesthesia panels, respectively.

Table 1.

Regions of interest.

ROI	ROI abbrev.
Auditory core:	
Heschl's gyrus, posterolateral	HGPM
Superior temporal plane (STP):	
Heschl's gyrus, anterolateral	HGAL
Planum temporale	PT
Planum polare	PP
Superior temporal gyrus (STG):	
Superior temporal gyrus, posterior	STGP
Superior temporal gyrus, mid	STGM
Superior temporal gyrus, anterior	STGA
Auditory-related:	
Insula	Ins
Superior temporal sulcus	STS
Middle temporal gyrus, posterior	MTGP
Middle temporal gyrus, mid	MTGM
Middle temporal gyrus, anterior	MTGA
Supramarginal gyrus	SMG
Angular gyrus	AG
Prefrontal:	
Inferior frontal gyrus, pars opercularis	IFGop
Inferior frontal gyrus, pars triangularis	IFGtr
Inferior frontal gyrus, pars orbitalis	IFGor
Middle frontal gyrus	MFG
Superior frontal gyrus *	SFG
Orbital gyrus	OG
Transverse frontopolar gyrus	TFG
Cingulate gyrus, anterior *	CGA
Sensorimotor:	
Precentral gyrus	PreCG
Postcentral gyrus	PostCG
Other:	
Premotor cortex	PMC
Parahippocampal gyrus	PHG
Fusiform gyrus	FG
Inferior temporal gyrus	ITG
Temporal pole	TP

ROI	ROI abbrev.
Gyrus rectus	GR
Superior parietal lobule *	SPL
Middle occipital gyrus	MOG
Inferior occipital gyrus *	IOG
Lingual gyrus *	LG
Cingulate gyrus, mid *	CGM
Amygdala	Amyg
Hippocampus	Hipp

* Limited coverage (present in 1 or 2 subjects out of 5)